Effect of Countermeasures for Pile Foundation Using Seismic Isolation Rubber during Liquefaction

K. Uno & M. Mitou
Institute of Technology, Penta-Ocean Construction Co., Ltd., Japan

H. Otsuka
Department of Civil and Structural Engineering, Kyushu University, Japan

SUMMARY:
During earthquakes, pile foundations are heavily damaged at the boundaries of soil layers, liquefiable and non-liquefiable ground, thereby leading to potential pile collapse. The intermediate part of the pile, which is the boundary division of liquefiable soil, is subjected to section force, and hence, in certain cases, the intermediate part of the pile has a greater risk of failure than the pile head. The seismic inertial force that increases the risk of collapse of piles during liquefaction is also clarified. The utility of the seismic resistance method for pile foundation that uses seismic isolation rubber in the intermediate part of the pile is demonstrated.

Keywords: pile foundation, liquefaction, seismic isolation rubber, shaking table test, effective stress analysis

1. INTRODUCTION

During an earthquake, pile foundations during liquefaction can be significantly damaged at the boundary division of liquefiable and non-liquefiable ground because of the inertial force of the corresponding superstructure, liquefaction, and lateral flow. Consequently, such piles can potentially collapse. Several previous earthquake surveys have observed such pile damage.

In the earthquake that occurred off the Pacific coast of Tohoku on March 11, 2011, liquefaction occurred in Urayasu, which is located in the Tokyo Bay area, as well as in the Miyagi, Fukushima, and Tochigi prefectures. The pile foundations in these areas appeared to have been damaged by liquefaction. In Onagawa in the Miyagi prefecture, a pile was extracted from the soil by a tsunami. The main cause of the pile collapse was the enormous tsunami waves, and it appears that the pile resistance to the tsunami was minimal because the ground around it had become loose.

Liquefaction mitigation for pile foundations can lead to considerable ground improvement. Furthermore, structural countermeasures, increased pile size, and the use of sheet piles can decrease the section force during an earthquake.

We conducted a shaking table test with a pile to understand the mechanism that damages the pile and the effects of soil liquefaction and inertial force on the pile. We consequently confirmed that a local section force was exerted on the pile at the layer boundary of liquefiable and non-liquefiable ground.

Subsequently, we developed seismic resistance in the pile foundation by using seismic isolation rubber at the place where the section force was found to be exerted, i.e., at the intermediate part of the pile.

2. OUTLINE OF EXAMINATION

2.1. Scale size and similarity rule

We first conducted the test with a normal pile, and then compared its results with those of the pile test with seismic isolation rubber.

Through these experiments, we hoped to achieve an essentially realistic model, and on its basis as well as by referencing existing literature, build a scale model. In our experiments, the pile was made of steel. The section parameters of the steel pipe pile are listed in Table 1.

A cross-section diagram of the test model is shown in Figure 1. The properties of the steel pipe piles in both the experiments were the same, except for the seismic isolation rubber that was used at the intermediate part of the pile only in the second experiment. The scale size of the model is 1/20 for both the modeling area and the size of the soil container. As can be seen in Table 2, we used the similarity rule for a 1 g gravitational field, as proposed by Iai (1988). It is calculated on the basis of an equation that governs the material phenomenon, and is roughly divided into that for saturated ground, structure (pile or sheet pile), and water. The length parameter is assumed to be a standard of the reduced scale of the similarity rules required by these sub-equations, and the reduced scale ratio of the other parameters is calculated accordingly. The similarity rule for soil fraction particle frame of the ground corresponds to the result of the study by Kagawa (1978) and Kokusho *et al* (1979).

Table 1. Section performance of a steel pipe pile

mejor diameter	(mm)	800	
pipe pile wall thickness	(mm)	12	9
corrosion allowance	(mm)	2.0	
cross-section area	(cm^2)	246.9	173.5
second moment of area	(cm^4)	190000	135000
section modulus	(cm^3)	4790	3390

Table 2. List of scaling law factors

Parameter	Scaling law	prototype/model
length	λ	20
density	1	1
time	$\lambda^{0.75}$	9.46
stress	λ	20
water pressure	λ	20
siaplacement	$\lambda^{1.5}$	89.4
acceleration	1	1
strain	$\lambda^{0.5}$	4.47
permeability	$\lambda^{0.75}$	9.46
bending stiffness	$\lambda^{4.5}$	715,542
axial stiffness	$\lambda^{2.5}$	1,789

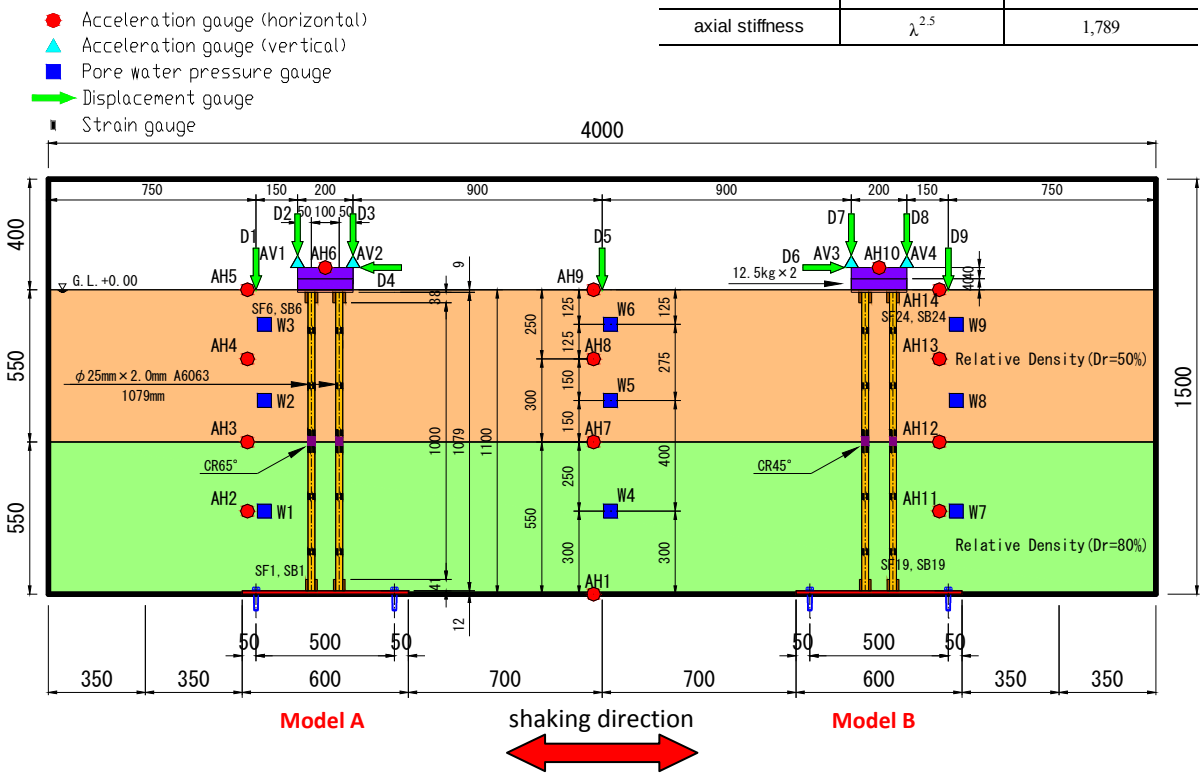

Figure 1. Cross-section drawing of the experiment model

The scale model was used to experimentally investigate the use of water. The effect of water viscosity on water penetration of the ground was determined by observing the dispersal of pore water pressure for a certain amount of time after the shaking test. The experimental results revealed that the water viscosity does not influence water penetration considerably during the test. Therefore, normal water was used in the experiments.

To observe the behavior of a pile during the shaking experiment conveniently, the number of piles was set to four. Because of the limitations of the experimental equipment, the length of each pile was reduced, even though the length requirement conformed to the similarity rule. In fact, even though we preferred the use of the steel pipe pile in this study, an aluminum pipe was used instead because of the similarity rule.

Furthermore, in order to observe the influence of the inertial force during an earthquake on behavior, the weight for obtaining the desired ratio of pile load to shear of the superstructure and substructure of the bridge was set to 25 kg.

2.2. Underwater shaking table and soil container

A large-scale underwater shaking table with a diameter of 5.5 m was used as the shaking test device. The experimental soil container had a box-type steel frame 4.0 m long, 1.5 m high, and 1.5 m deep. To prevent the water from flowing back into the soil container, the outflow and inflow of water from the soil container boundary were enabled by attaching an unwoven cloth to the expanded metal perpendicular to the shaking direction. The shaking table was mounted on a water pool 15 m long, 15 m wide, and 2 m deep.

2.3. Model development

First, the plate and the shaking table installed in the pile in the soil container were fixed with a bolt. The pile was then inserted in a ring welded to the plate; the ring was fixed in two directions with bolts. Further, an epoxy resin was injected into the space between the ring and the pipe. The setting of the pile foundation is shown in Figure 2. Next, non-liquefiable and liquefiable ground were prepared using Soma sand. The non-liquefiable layer reached the prescribed height at a relative density of 80%, and the soil was compacted and flattened. The density of the sand was determined using the weight and height of the ground for every 100 mm thick layer.

Figure 2. Setting situation of the pile foundation

The non-liquefiable layer was prepared in dry air. Water was then poured to form the liquefiable layer. The liquefiable layer, with a relative density of 50%, was prepared with sand by underwater sedimentation.

The materials used for preparing the pile foundation and soil are listed in Table 3, and the dimensions of the pile foundation model are listed in Table 4. As shown by both Tables 3 and 4, the steel plate connected to the top of the pile (which is usually the bridge footing section) is considered the upper structure, and the steel plate fixed at the bottom of the pile and the shaking table is considered the lower structure.

Table 3. List of the materials of the soil and the pile foundation

item		material	remarks
Liquefied ground		Soma-Sand (underwater sedimential method)	Dr≒50%
Non-liquefied ground		Soma-Sand (in air method)	Dr≒80%
Pile foundation	upper	steel plate	t=9mm
	lower	steel plate	t=12mm
	pile	aluminum pipe	φ=25mm, t=2.0mm

Table 4. Size of the pile foundation model

structure	detail	figure	material	measurement
Pile foundation	upper structure	plate	steel	PL-200×200×9
		ring	steel	42(mejor diameter)×8(wall thickness)×38(height) (minor diameter: 26mm)
	lower structure	plate	steel	PL-1100×600×12
		ring	steel	46(mejor diameter)×10(wall thickness)×41(height) (minor diameter: 26mm)
	pile	pile	aluminum	25(major diameter)×2.0(wall thickness)×1079(length) (minor diameter: 21mm)
Weight	-----	plate	steel	PL-200×200×4

2.4. Seismic isolation rubber

Seismic isolation rubber was installed at the intermediate part of the pile, as shown in Figure 1. The configuration of the seismic isolation rubber and its method of installation in the pile are shown in Figure 3. The seismic isolation rubber was not a laminated structure but a unit. Two hardness values (CR65° and CR45°) were obtained at the layer boundary of the intermediate part of the pile. Further, the pile and rubber were fixed using adhesive. The pile with hardness of CR65° was labeled Model A and that with hardness of CR45° was labeled Model B.

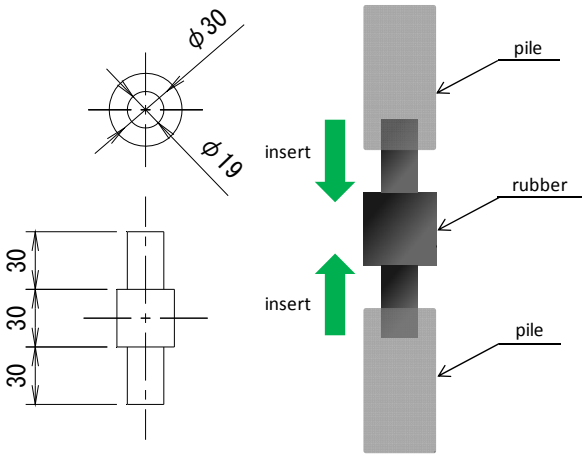

Figure 3. Configuration of the seismic isolation rubber and the installation method to the pile (unit: mm)

2.5. Shaking wave

First, shaking tests were conducted under the conditions of a 1 g sinusoidal wave with a frequency of 10 Hz and a wavenumber of 20. The frequency was set in consideration of the natural period for pile foundation and the frequency that influenced structures in previous earthquakes.

In our experiments, we studied two cases—one with 100 Gal (Case 1, shown in Figure 4) and the other with 350 Gal (Case 2). A taper was installed in the first wave in each of the tests.

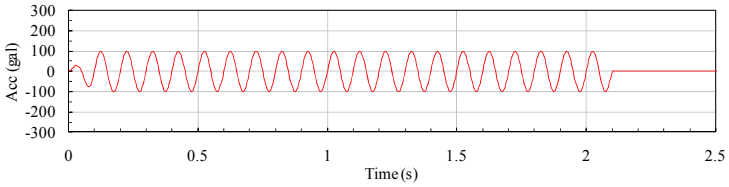

Figure 4. Shaking wave (100 Gal)

Next, we conducted shaking tests with seismic waves. Inland-type earthquake motions were computed from the records of the Kobe Port Island strong-motion seismographs during the Southern Hyogo Prefecture Earthquake as an earthquake motion in a release base (Figure 5).

Trench-type earthquake motions were computed as a simulated earthquake motion waveform in the release base, which is located near the fault for the fault model of the assumed Tokai earthquake advocated by the Central Disaster Prevention Council (Figure 6).

The level-2 inland-type earthquake motion and the ocean trench-type (plate boundary-type) earthquake motion, which have been specified in the Standard Specifications for Concrete Structures (2002), Seismic Performance Verification, were used.

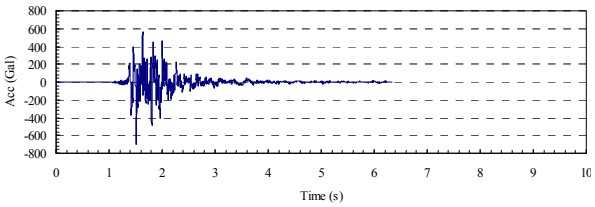

Figure 5. Shaking wave
(Kobe Port Island strong-motion seismograph record)

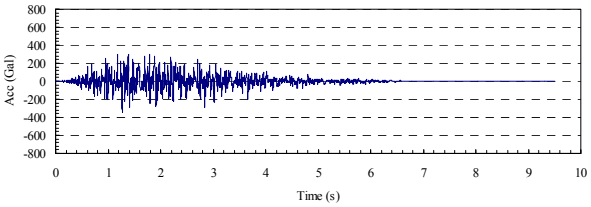

Figure 6. Shaking wave
(Supposed Tokai Earthquake Fault model)

3. OUTLINE OF REPLICATE ANALYSIS OF EXAMINATION

3.1. Analysis conditions

An effective stress analysis for replicating the shaking table tests was conducted by using the analysis code FLIP. The parameters used for this analysis are listed in Table 5. Liquefaction and non-liquefying layers were modeled with a multiple-shear spring element. The pile and footing sections were modeled with a linear beam element. In addition, the cross-sectional rigidity, density, and weight of the footing part were also taken into consideration. Seismic isolation rubber, whose modeling is explained in detail in the next section, was modeled with a linear spring element. The other parameters were set on the basis of the standard method of FLIP. For the boundary condition, the side of the soil container was modeled with a perpendicular roller, and its bottom was modeled on the fixed boundary.

Furthermore, in FLIP, the rigid proportionality coefficient β was applied by using Rayleigh damping

Table 5. Parameters of analysis model

classification	dynamic deformation characteristics parameter										
	density ρ (t/m^3)	confining pressure σ_{ma}' (kN/m^2)	shear modulus G_{ma} (kN/m^2)	bulk modulus K_{ma} (kN/m^2)	m_G	m_K	Poisson's ratio ν	porosity n	cohesion c (kN/m^2)	internal friction angle φ_f (°)	maximum damping ratio h_{max}
liquefaction	1.88	1.61	9,212	24,023	0.5	0.5	0.33	0.467	0	36.7	0.24
non-liquefaction	1.94	4.95	12,416	32,379	0.5	0.5	0.33	0.426	0	42.1	0.24

classification	liquefaction characteristics parameter					
	phase transformation angle φ_p (°)	S1	W1	P1	P2	C1
liquefaction	28	0.005	2.244	0.5	1.07	1.815
non-liquefaction	—	—	—	—	—	—

as a rigid proportionality type for the calculation of stabilization; in addition, we propose the method of estimating beta at the maximum value of the response displacement convergence of the one-dimensional nonlinear soil. This analysis can also set the value of beta to 0.001 by using the above-mentioned technique. After conducting a dead weight analysis, we carried out a dynamic response analysis in order to reproduce an initial stress state.

3.2. Modeling of seismic isolation rubber

In this analysis, because seismic isolation rubber was modeled with a linear spring element, the spring constant is computed by using the following methods:

The spring constant of rubber K is given by the following formula:

$$K = \frac{W}{\delta} = \frac{E_{ap} \times A_L}{h} \tag{3.1}$$

where
W : load (N), δ : flexure (cm), E_{ap} : apparent Young's modulus (MPa)
A_L : area of pressure surface (cm^2), h : height of rubber (cm)

The value of the apparent Young's modulus varies with the influence of the rubber form, and it is calculated by using the following formula on the basis of the cylinder form:

$$E_{ap} = G_s \left(3 + 4.94 S^2\right) \tag{3.2}$$

where
G_s : shear modulus of rigidity (MPa), S : ratio of configuration

Moreover, in the case of a cylinder, the ratio of the configuration in Eqn. (3.2) is obtained using the following formula:

$$S = d/4h \tag{3.3}$$

where
d : diameter, h : height

The shear modulus of rigidity and the type and hardness of rubber are correlated. The shear modulus of rigidity of CR65° is approximately 1.25 MPa, and that of CR45° is approximately 0.60 MPa.

As mentioned above, we could estimate the spring constant of rubber when CR65° was 36.9 kN/m and CR45° was 17.7 kN/m.

Further, while the rocking behavior of rubber cannot be assumed, the perpendicular spring constant and the rotation spring constant can be estimated by assuming a considerable value of rigidity.

4. RESULTS OF EXAMINATION AND ANALYSIS

Although we mention the reproducibility of the experimental results and analysis in this paper, because of space limitations, we mainly discuss the acceleration and the excess pore water pressure of a pile head.

The time histories of the response acceleration of the pile head and the excess pore water pressure ratio of the liquefied ground are shown in Figures 7 and 8.

For Case 1, although the method for increasing excess pore water pressure during shaking in the experiment is different from that in the analysis, when the seismic isolation rubber acts after complete liquefaction, we observe that the experimental result are reproducible.

For Case 2, the experimental result is mostly reproducible with the considered analysis techniques, such as the timing of the increase in water pressure and the acceleration response obtained at the beginning of shaking.

The time histories of the response acceleration of the pile head and the excess pore water pressure ratio of the liquefaction ground in the case of the input seismic waves are shown in Figures 9 and 10.

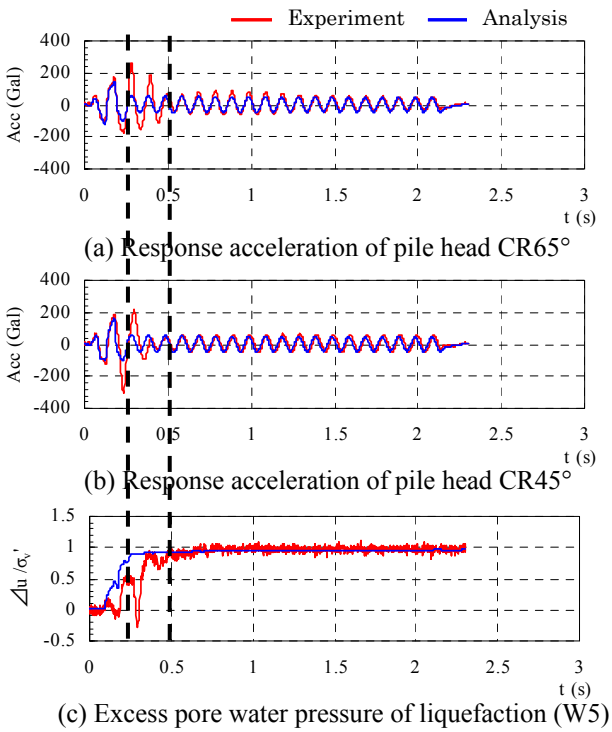

Figure 7. Results of Case 1

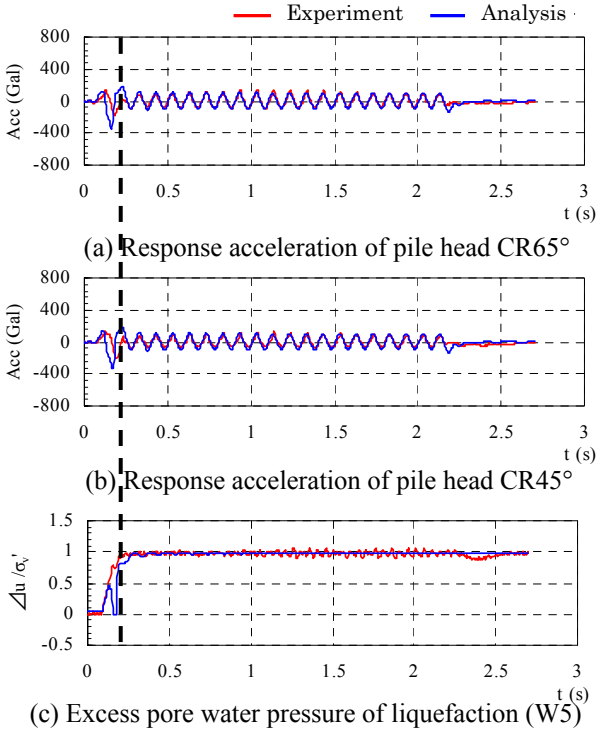

Figure 8. Results of Case 2

Although the experimental and analytical results vary slightly with respect to increased water pressure in the case of an inland-type earthquake motion and an ocean trench-type earthquake motion, the time taken for complete liquefaction is almost the same for both the analysis and the experiment; hence, the experiment is reproducible.

Furthermore, with respect to the time histories of acceleration, both the cases can be reproduced in most of the experiments, such as those involving acceleration level and the time history form.

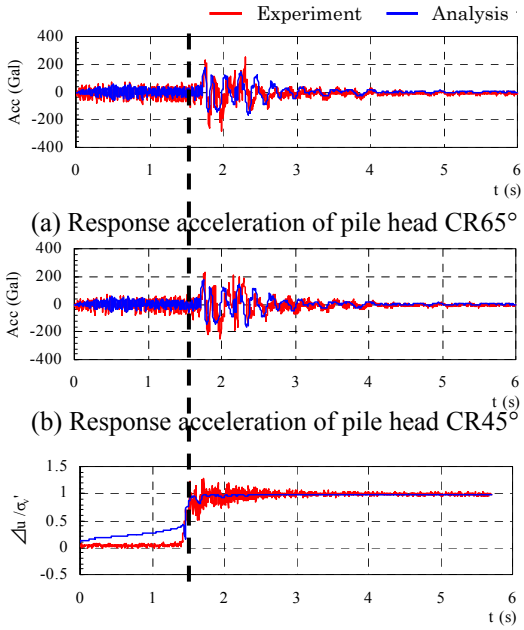

(a) Response acceleration of pile head CR65°

(b) Response acceleration of pile head CR45°

(c) Excess pore water pressure of liquefaction (W5)

Figure 9. Results of Kobe PI Earthquake

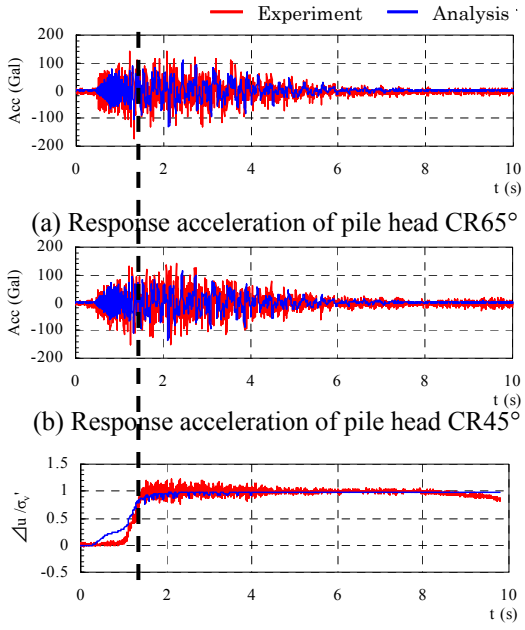

(a) Response acceleration of pile head CR65°

(b) Response acceleration of pile head CR45°

(c) Excess pore water pressure of liquefaction (W5)

Figure 10. Results of Tokai Earthquake

5. POSSIBILITY OF COUNTERMEASURE FOR LATERAL FLOW

We confirm that the pile foundation system using seismic isolation rubber we developed is effective not only liquefiable ground but also lateral flow ground with liquefaction.

A cross-section diagram of the test model is shown in Figure 11. The properties of the steel pipe piles are the same as the previous liquefaction experiment. The scale size of the model is 1/20 for the modeling area and the size of the soil container. As can be seen in Table 2, we use the similarity rule for a 1 g gravitational field.

The number of piles is set to four, and in order to observe the influence of the inertial force during an earthquake on behavior, the weight is set to 25 kg.

The model makes it possible to produce a lateral flow phenomenon by installing the steel plate which simulated sheet pile quay wall in the front side of the pile foundation.

Non-liquefiable and liquefiable ground are prepared using Iide sand. By the Great East Japan Earthquake, because a sand extraction of Soma sand is in Fukushima, we had to change the sand kind. So we use Iide sand gotten in Yamagata in this experiment.

Shaking test is conducted under the conditions of a 1 g sinusoidal wave with a frequency of 10 Hz and a wavenumber of 20. In our experiments, we study the case with 350 Gal. A taper was installed in the first wave in each of the tests.

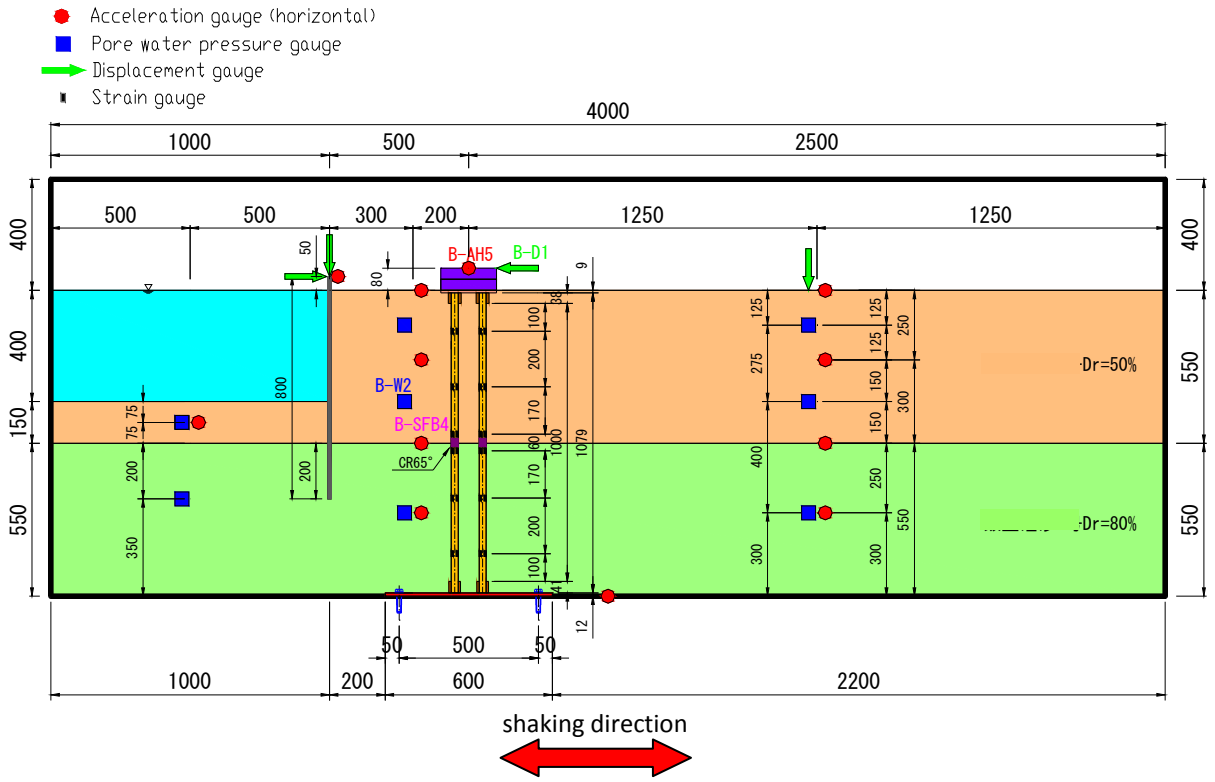

Figure 11. Cross-section diagram of the lateral flow experiment model

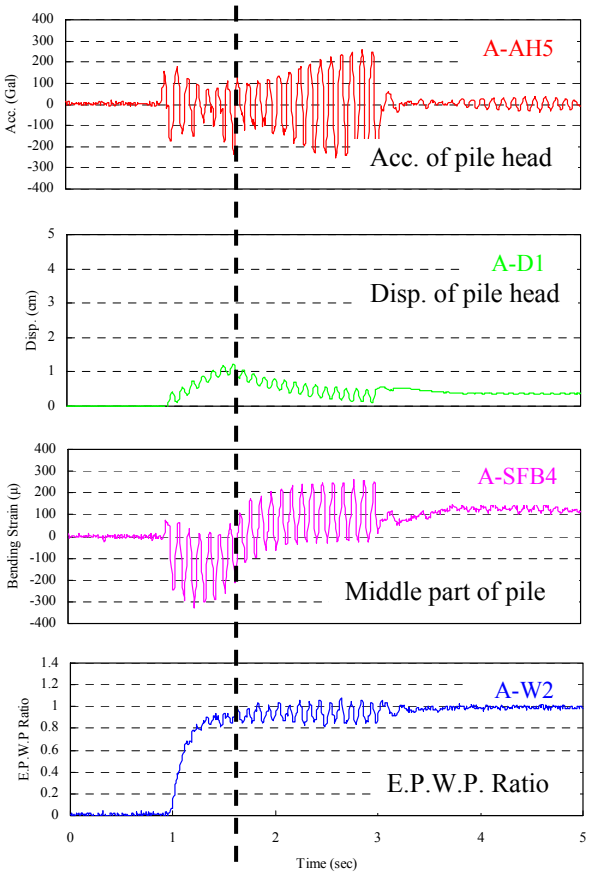

Figure 12. Time histories of normal pile

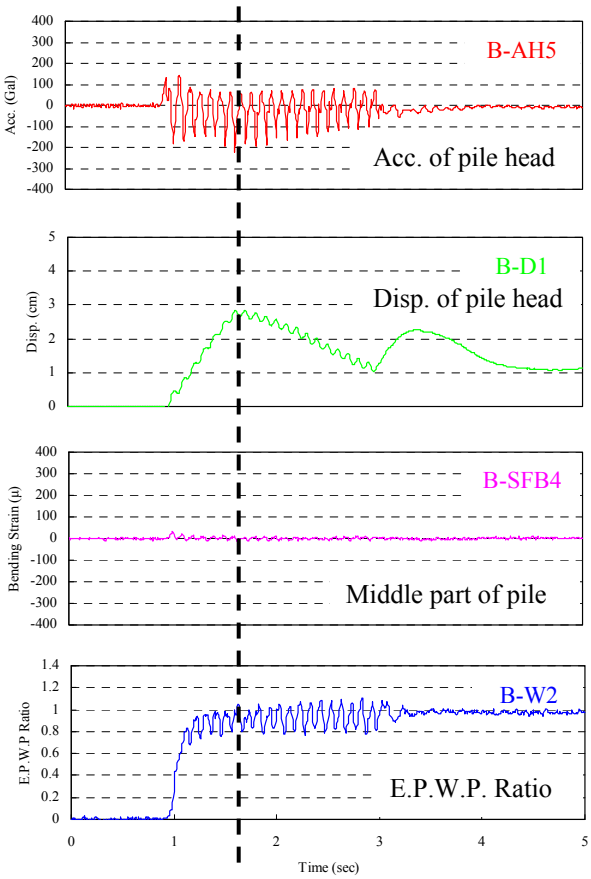

Figure 13. Time histories of seismic isolation pile

The results of normal pile are shown in Figure 12, and the results of the pile using seismic isolation rubber (seismic isolation pile) are shown in Figure 13. In this experiment, the stopper which prevents the steel plate from being collapse. During shaking, at the time of 1.6 second after beginning of record, the steel plate hits the stopper. So we discuss the results about the time before 1.6 seconds. The seismic isolation pile shows longer displacement than the normal pile one. So it is not appropriate to apply the seismic isolation pile at the place where the pile and the quay wall are very close to each other. But the bending strain of the seismic isolation pile is decreased, so it is contemplated that the risk of failure to the intermediate part of pile is descended.

6. CONCLUSIONS

Pile foundations in liquefied soils are likely to be heavily damaged at the boundary between liquefied soil layer and non-liquefied soil layer during an earthquake because of the inertial force of a superstructure, liquefaction, and lateral flow. Consequently, there is a possibility that the piles will collapse. Such pile damages have been observed in surveys conducted for past earthquakes. So far, we have conducted a shaking table test with a pile to understand the mechanism that damages the pile and the effects of soil liquefaction and inertial force on the pile. We confirmed through the test that a local section force is exerted on the pile at the layer boundary.

In this study, in order to develop a structure with seismic resistance, seismic isolation rubber was applied to the intermediate part of a pile. In an earlier study, we demonstrated in a shaking table test that the seismic isolation rubber is very effective because the section force in the middle part of the pile decreased. So in order to check the validity of the modeling of the seismic isolation rubber in the effective stress analysis of the pile foundation, a reappearance analysis of the shaking table test was carried out; it was shown that the performed experiments were mostly reproducible using this analysis technique.

ACKNOWLEDGEMENT

For help with determining the characteristics of the seismic isolation rubber and performing the shaking test method, the authors express their gratitude to Dr. Hiroo Shiojiri (Professor, College of Science and Technology, Nihon University) for his guidance and advice. We thank Mr. Hamagami and Mr. Sasaki of the Yokohama Rubber Co., Ltd. for providing the experimental materials and the seismic isolation rubber.

REFERENCES

Uno, K., Otsuka, H. and Mitou, M. (2011). The consideration about the seismic resistance improvement of the bridge pile foundation with the seismic isolation system in liquefied ground, *Japan Society of Civil Engineers 2011 Annual Meeting*, **I-503** (in Japanese)

Uno, K., Otsuka, H. and Mitou, M. (2011). Experimental study on influence of soil liquefaction and seismic inertial force on bridge pile foundation, *Annual Meeting of Kanto Branch of JSCE*, **I-35** (in Japanese)

Iai, S. (1988). Similitude for Shaking Table Tests on Soil-Structure-Fluid Model in 1g Gravitational Field, *Report of the Port and Harbour Research Institute*, **Vol.27**, No.3

Kagawa, T. (1978). On the similitude in model vibration tests of earth-structures, *Proceedings of the Japan Society of Civil Engineers*, **No.275**, 69-77 (in Japanese)

Kokusho, T. and Iwatate, T. (1979). Scaled model tests and numerical analyses on nonlinear dynamic response of soft grounds, *Proceedings of the Japan Society of Civil Engineers*, **No.285**, 57-67 (in Japanese)

National Institute for Land and Infrastructure Management and Incorporated Administrative Agency, Public Works Research Institute (2011). Quick Report on Damage to Infrastructures by the 2011 off the Pacific coast of Tohoku Earthquake, *Technical Note of National Institute for Land and Infrastructure Management*, **No.646** (in Japanese)

Japan Society of Civil Engineers (2002). Standard Specifications for Concrete Structures-2002, Seismic Performance Verification (in Japanese)

Iai, S., Matsunaga, Y. and Kameoka, T. (1992). Analysis of Undrained Cyclic Behavior of Sand under Anisotropic Consolidation, *Soils and Foundations*, **Vol.32**, 16-20